Cite this: *Phys. Chem. Chem. Phys.*, 2012, **14**, 9306–9310

www.rsc.org/pccp

PAPER

A computational study on the intriguing mechanisms of the gas-phase thermal activation of methane by bare $[Ni(H)(OH)]^+$ †

O. Lakuntza,[a] J. M. Matxain,[a] F. Ruipérez,[a] M. Besora,[b] F. Maseras,[bc] J. M. Ugalde,*[a] M. Schlangen[d] and H. Schwarz*[de]

Received 7th November 2011, Accepted 16th January 2012
DOI: 10.1039/c2cp23502a

A detailed computational study on the reaction mechanisms of the thermal activation of methane by the bare complex $[Ni(H)(OH)]^+$ has been conducted. The experimentally observed reaction features, *i.e.* the ligand exchange Ni(H) → $Ni(CH_3)$, the H/D scrambling between the incoming methane and the hydrido ligand of the nickel complex, the spectator-like behavior of the OH ligand, and the relatively moderate reaction efficiency of 6% relative to the collision rate of the ion/molecule reaction, can be explained by considering three competing mechanisms, and a satisfactory agreement between experiment and theory has been found.

Introduction

The activation and functionalization of methane under ambient conditions remain a challenge in contemporary chemistry.[1] Among the numerous gas-phase studies aimed at elucidating mechanistic aspects of the C–H bond activation by using bare or ligated transition-metal ions or by employing small metallic cluster species, the thermal reaction of $[Ni(H)(OH)]^+$ (**1**) with CH_4, eqn (1),[2] has received quite some attention.

$$[Ni(H)(OH)]^+ + CH_4 \rightarrow [Ni(CH_3)(OH)]^+ + H_2 \quad (1)$$

Pertinent findings of this ion/molecule reaction are: (1) the hydroxy group does not participate but rather acts as a spectator ligand and (2) partial H/D exchange of the hydrido ligand with the incoming hydrocarbon occurs prior to or during the formation of the nickel–carbon bond. Modeling of the extensive labeling experiments reveals that *direct* hydrogen/methyl ligand exchange amounts to 46%, while 54% of the encounter complex undergoes H/D scrambling prior to loss of molecular hydrogen. For the former process the kinetic isotope effect (KIE) amounts to 1.9, and for the latter KIE = 1.4, thus suggesting that breaking of the nickel–hydrogen and carbon–hydrogen bonds is involved in the rate-limiting step. The electronic structure of the reagent $[Ni(H)(OH)]^+$ also turned out to be of quite some interest.[3,4] For example, the doublet state of $[Ni(H)(OH)]^+$ is *ca.* 1 eV more stable than its quartet electromer and is further found to readily undergo a near barrier-free reductive elimination to afford $^2[Ni(H_2O)]^+$; this Ni^I–H_2O complex is thermodynamically stable and kinetically inert toward CH_4.[2] The observed gas-phase reactivity of $^4[Ni(H)(OH)]^+$ is due to the fact that the hydroxyl group of this complex behaves actually as a redox non-innocent ligand resulting in an electronic structure which is consistent with a $^4[(H)Ni^{II}–(OH^{\bullet})]^+$ species rather than a formally resonant $^4[(H)Ni^{III}–(OH^-)]^+$ system. As a consequence of the electronic structure mismatch there is no direct, facile way of converting this high-energy quartet electromer to the ground-state doublet by a simple spin flip; rather, an insufficient combination of metal-to-ligand electron transfer followed by a spin inversion is operative[3b] thus providing a kinetic protection of the quartet state and imparting to it a lifetime long enough to undergo the thermal ion/molecule reaction with CH_4.[2,3b]

Here, we will present a computational study which addresses the hitherto unknown mechanistic details of the experimentally observed partial H/D exchange between the hydrido ligand of $^4[Ni(H)(OH)]^+$ and CH_4. The computations are confined to the quartet state of the nickel complex based on the grounds outlined above.[2,3]

Computational details

All calculations were performed using the hybrid density functional theory functionals B3LYP[5] and M06[6] with triple-ζ plus polarization basis sets TZVP for the nickel atom.[7]

[a] *Kimika Fakultatea, Euskal Herriko Unibertsitatea, and Donostia International Physics Center (DIPC), P.K. 1072, 20080 Donostia, Euskadi, Spain. E-mail: jesus.ugalde@ehu.es*
[b] *Institute of Chemical Research of Catalonia (ICIQ), Av. Països Catalans, 16, 43007 Tarragona, Catalonia, Spain*
[c] *Departament de Química, Edifici Cn, Universitat Autónoma de Barcelona, 08193 Bellaterra, Catalonia, Spain*
[d] *Institut für Chemie, Technische Universität Berlin, Straße des 17. Juni 115, 10623 Berlin, Germany. E-mail: Helmut.Schwarz@mail.chem.tu-berlin.de*
[e] *Chemistry Department, Faculty of Science, King Abdulaziz University, Jeddah 21589, Saudi Arabia. E-mail: hschwarz@kau.edu.sa*

† Dedicated to Professor Ludger Wöste on the occasion of his 65th birthday.

Frequency calculations, at the same level of theory, were performed to characterize stationary points and to estimate harmonic zero-point vibrational energy (ZPVE) corrections. The latter have been included in the reported relative energies (given in eV). The TZVP basis set was supplemented with a diffuse *s* function, two sets of *p* functions (optimized by Wachters[8]) for the excited states, one set of diffuse pure *d* angular momentum functions (optimized by Hay[9]), and three sets of uncontracted pure angular momentum *f* functions, including both tight and diffuse exponents, as recommended by Raghavachari and Trucks.[10] For the oxygen, carbon and hydrogen atoms, the 6-311++G(3df,2p) basis set (denoted as TZVP+G(3df,2p)) reported by Krishnan *et al.* was used.[11] For selected aspects, we have also carried out CCSD(T) single-point calculations using the B3LYP optimized structures, and in very few cases, quite demanding CCSD geometry optimizations were performed.[12] For all calculations we have used the GAUSSIAN03[13] and the NWChem5.1[14] suite of programs. Previous studies showed[3,15] that the B3LYP and M06 hybrid functionals together with a TZVP+G(3df,2p) basis set are a good choice for a qualitative description of the problem at hand in that the energetic differences between experimental and computational data in general do not exceed ±0.3 eV.

For the location of the minimum energy crossing points (MECPs), which are relevant in two-state reactivity (TSR) scenarios,[16] we treated the present system in a pseudo-one-dimensional way; here, each of the two crossing surfaces are mapped out for several values of a given reaction co-ordinate, which is typically a bond length or a bond angle. The crossing point between the resulting one-dimensional curves is a rough approximation to the lowest energy crossing point between the surfaces. However, it is usually more accurate, and faster, to use a gradient-based method to explicitly locate the exact minimum energy crossing point between the surfaces. Several algorithms have been proposed in the literature.[17] In this work, we have used a script program to locate and characterize the MECPs. This program (a) generates suitable input files for an electronic structure code, (b) calls the code, (c) extracts from the output the energies and gradients on two surfaces, (d) combines them to yield an effective gradient which is directed towards the MECP, and (f) uses it to update the geometry until convergence is achieved.

Results and discussion

In Fig. 1 we present the simplified potential energy surface (PES) for the ligand exchange according to eqn (1). The reaction commences with the exothermic barrier-free formation of the encounter complex **2** which is characterized by a η^2-coordination of the incoming methane molecule. For **2** various conformers, *e.g.* rotation around the Ni–OH bond, exist which are separated by barriers much below the σ-metathesis transition state **TS2/3**. In this σ-complex assisted reaction[18] the emerging H_2 molecule of **TS2/3** has a bond length of 1.001 Å. **TS2/3** leads directly to the ion/molecule complex $^4[(H_2)Ni(CH_3)(OH)]^+$ (**3**); here, formation of the H_2 leaving group is nearly complete as indicated by the close-to-equilibrium bond length of 0.766 Å. From **3**, liberation of H_2 proceeds without a barrier to form the ligand-exchange product

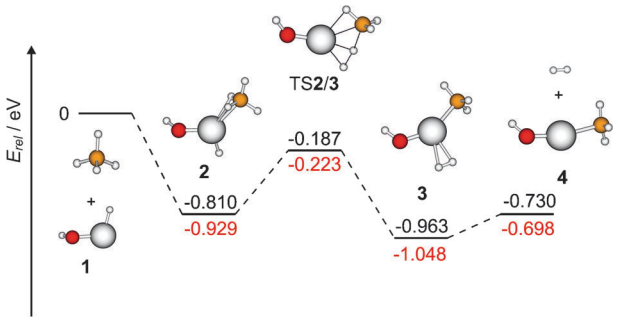

Fig. 1 B3LYP (in black) and M06 (in red)/TZVP+G(3df,2p) derived potential energy surfaces for the σ-metathesis reaction of $^4[Ni(H)(OH)]^+ + CH_4 \rightarrow {}^4[Ni(CH_3)(OH)]^+ + H_2$. Relative and ZPVE corrected energies are given in eV.

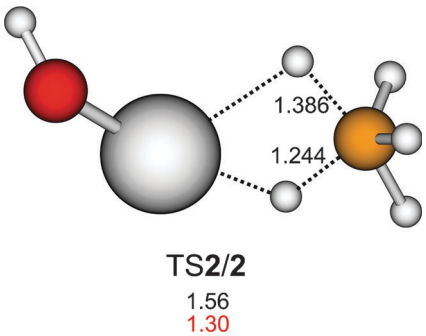

Fig. 2 Geometrical details (B3LYP) of the hydrogen exchange transition state **TS2/2**. ZPVE corrected energies are related to the entrance channel and given in eV (B3LYP in black and M06 in red).

$^4[Ni(CH_3)(OH)]^+$ (**4**). The overall reaction is exothermic by −0.730 eV (B3LYP) and −0.698 eV (M06); the entropy contribution to the reaction at room temperature is not significant as indicated by $\Delta G = -0.647$ eV (as compared to $\Delta E = -0.730$ eV). As the crucial **TS2/3** and the exit channel are located well below the entrance channel and as the reaction is not subject to a spin change its smooth occurrence under thermal conditions is expected.

However, the experimentally observed specific hydrogen exchange between the Ni–H unit of **1** and the incoming methane ligand cannot be explained in terms of Fig. 1. In a rather extensive search of the PES, we managed to locate a transition state **TS2/2** (Fig. 2) in which, starting from **2**, a degenerate H/H exchange is possible (**2** ⇄ **TS2/2**); however, as this transition state is located 1.56 eV (1.30 eV with M06) above the entrance channel it cannot account for the observed thermal H/D exchange that precedes or accompanies the hydrogen/methyl ligand exchange in the couples $[Ni(H)(OH)]^+/CD_4$ and $[Ni(D)(OH)]^+/CH_4$.

In our computational search for a reaction path which may account for the H/D scrambling we did not only eventually succeed but came across also an entirely unexpected route for the H/CH_3 ligand exchange which is energetically even more favorable than the σ-metathesis path described in Fig. 1. In this new reaction, Fig. 3, the encounter complex **2** rearranges *via* **TS2/5** to an almost linear dihydrogen-bridged complex **5**. In **5**, the bond length of the central H–H unit amounts to 1.027 Å (B3LYP), thus indicating the incipient formation of a

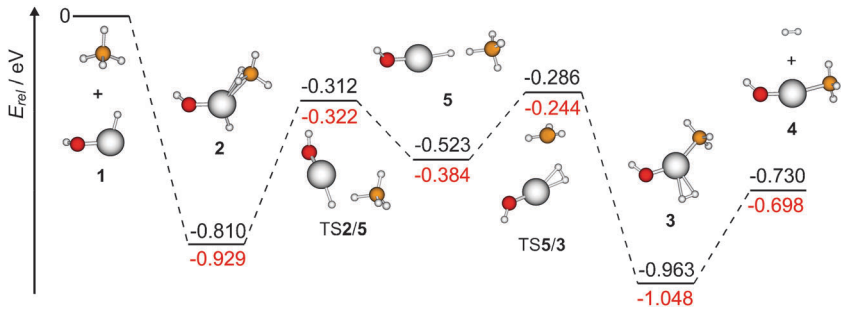

Fig. 3 B3LYP (in black) and M06 (in red)/ZVP+G(3df,2p) derived potential energy surfaces for the indirect H/CH_3 ligand exchange in the couple ^{4}[Ni(H)(OH)]$^+$/CH_4. Relative and ZPVE corrected energies are given in eV.

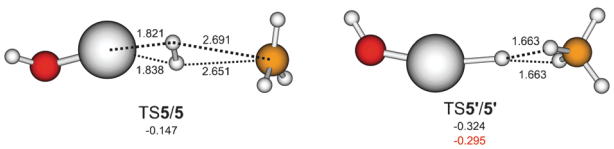

Fig. 4 Geometrical details (B3LYP) of the transition states **TS5/5** and **TS5′/5′** involved in the hydrogen exchange. ZPVE corrected energies are related to the entrance channel and given in eV (B3LYP in black and M06 in red). **TS5/5** could not be located using M06.

hydrogen–hydrogen bond as compared to **TS2/5** having an H–H bond length of 1.276 Å. Similarly, the C–H bond of methane involved in making the central H–H motif gets elongated from 1.189 Å (**TS2/5**) to 1.232 Å; the same trend is observed for the Ni–H bond which varies from 1.589 Å (**2**) *via* 1.667 Å (**TS2/5**) to 1.751 Å (**5**). From intermediate **5**, in a complex motion *via* **TS5/3** involving migration of the terminal CH_3 group to the nickel center and rotation of the internal H–H unit, the side-on (H_2) complex **3** is formed. We note that in **TS5/3** the H–H distance is significantly shortened to 0.829 Å. Interestingly, the two transition states in this two-step pathway are energetically lower in energy than the one for the direct σ-complex assisted process depicted in Fig. 1, and thus may act as an efficient competitor. Moreover, starting from the linear intermediate **5**, hydrogen exchange is feasible under ambient conditions. To this end, in a combination of a scrambling transition state (**TS5/5**), which accounts for the positional exchange of the central H–H unit, and a rotation of the methane ligand *via* **TS5′/5′** (Fig. 4), exchange of the original hydrido ligand and a hydrogen atom from the incoming methane ligand can take place. While **TS5/5** is higher in energy than **TS2/5** and **TS5/3**, **TS5′/5′** has been located at similar energies; both **TS5/5** and **TS5′/5′** are still below the entrance energy (**TS5/5**: −0.147 eV at B3LYP and −0.319 eV at CCSD(T)/B3LYP, **TS5/5** could not be located using M06; **TS5′/5′**: −0.324 eV at B3LYP, −0.295 eV at M06, and −0.408 eV at CCSD(T)/B3LYP). Moreover, although the relative energies as obtained by B3LYP, M06 and the CCSD(T)/B3LYP calculations for the four crucial transition structures exhibit some differences (Table 1), the global picture is similar and the agreement is pleasing. By and large, the same holds true for the energetics of the species shown in Fig. 3.

Table 1 Relative energies (in eV) of the various transition structures related to [(H_3C)HHNi(OH)]$^+$ (**5**)

	B3LYP	M06	CCSD(T)/B3LYP
5	0.00	0.00	0.00
TS2/5	0.21	0.06	0.18
TS5/3	0.24	0.14	0.11
TS5′/5′	0.20	0.08	0.16
TS5/5	0.38	[a]	0.25

[a] **TS5/5** could not be located using the M06 functional.

Finally, we would like to address the experimental observation that the OH ligand of **1** remains "inert" in both the hydrogen exchange and the ligand switch reaction of the [Ni(H)(OH)]$^+$/CH_4 couple. A further PES screening of the encounter complex **2** reveals that in an unusual σ-metathesis process rearrangement to the formal Ni^{III}-complex ^{4}[Ni(H)(H_2O)(CH_3)] (**6**) *via* **TS2/6** is both kinetically and thermodynamically possible (Fig. 5). According to the PES depicted in Fig. 5, this water–nickel complex has two options: (i) an entropically favored liberation of H_2O to generate **7** and (ii) preceded by a near-barrier free rotation around the Ni–(OH_2) bond of **6**, hydrogen transfer from the water ligand *via* **TS6/3** to form the final complex **3**; from **3** H_2 is liberated to produce the ligand exchange product **4**. However, neither loss of water from the [Ni(H)(OH)]$^+$/CH_4 couple nor involvement of the OH ligand of **1** in the formation of H_2 are observed in the experiment.[2] How to reconcile the experimental with the computational findings? The answer is rather surprising.

In contrast to the reactions of ^{4}[Ni(H)(OH)]$^+$ with CH_4 as depicted in Fig. 1 and 3, in which the quartet state is clearly separated from the doublet state and therefore a spin change to the energetically more favorable doublet surface is highly unlikely to occur, the situation is fundamentally different after having formed **6**. Rather than undergoing loss of water (**6** → **7**) or engaging in hydrogen migration **6** → **3**, in the energetic vicinity of **6** we located a crossing point (0.143 eV at B3LYP, 0.071 eV at M06, and 0.074 eV at CCSD(T)/B3LYP relative to ^{4}**6**) that leads to the energetically extremely favored doublet state of [Ni(CH_4)(H_2O)]$^+$ which is *ca.* 3 eV more stable than ^{4}**6**. Thus, rather than proceeding along the reactions depicted in Fig. 5, ^{4}**6** prefers to isomerize to the inert ^{2}[Ni(H_2O)]$^+$/CH_4 complex, from which loosely bound CH_4 can easily evaporate.[2] The existence of this "exit" channel may also explain the somewhat lower ion/molecule reactivity of the [Ni(H)(OH)]$^+$/CH_4 couple as production of an inert product competes efficiently with the H/CH_3 ligand exchange, eqn (1). However, since **TS2/6** is higher in energy compared to **TS2/5** (0.059 eV at B3LYP and 0.112 eV at M06), dehydrogenation can successfully compete with the formation of unreactive ^{2}[Ni(H_2O)]$^+$/CH_4.

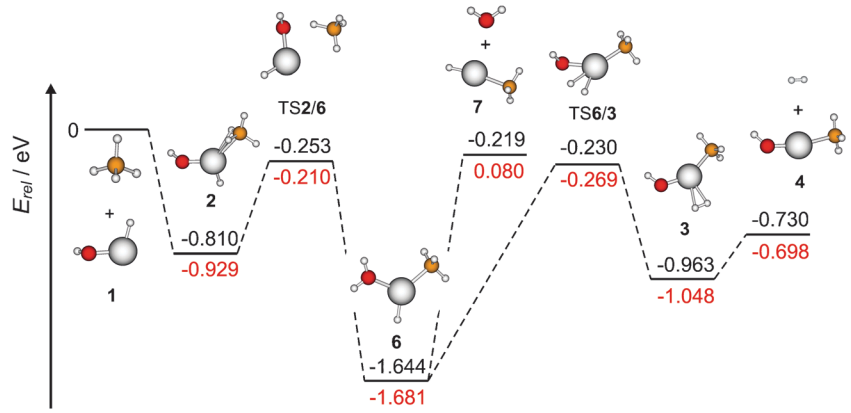

Fig. 5 B3LYP (in black) and M06 (in red)/ZVP+G(3df,2p) derived potential energy surfaces involving the OH ligand of $^4[Ni(H)(OH)]^+$ in the reaction with CH_4. Relative and ZPVE corrected energies are given in eV.

This coupled spin-inversion, isomerization reaction can be understood considering the electronic situation of $^4[Ni(CH_3)(H)(H_2O)]^+$, which has a spin density of 1.01 for the CH_3 group and 1.95 for Ni (B3LYP). In the spin-crossing process, one of the unpaired electrons of the nickel atom undergoes a spin flip while the carbon retains its single unpaired electron. Next, the methyl group behaving as a radical attacks intramolecularly the H–Ni bond leading to the formation of the doublet state of $[Ni(CH_4)(H_2O)]^+$. Thus, the presence of this MECP can explain the fact that the OH ligand remains intact along the ligand/hydrogen switch described in eqn (1).

Conclusions

We have identified computationally three reaction pathways that are relevant in the thermal activation of methane by the bare $[Ni(H)(OH)]^+$ complex. Our findings provide an explanation for the hydrogen exchange of the nickel hydrido ligand with the hydrogen of the incoming methane ligand that precedes the actual ligand switch $^4[Ni(H)(OH)]^+/CH_4 \rightarrow {}^4[Ni(CH_3)(OH)]^+ + H_2$. We further explain why the OH ligand remains inert in the hydrogen exchange process. Finally, the somewhat reduced efficiency of the thermal ion/molecule reaction is accounted for by an efficient quartet/doublet spin inversion that takes part of the $[Ni(H)(OH)]^+/CH_4$ population from the reactive quartet surface to the thermochemically much more stable doublet surface to produce "inert" $^2[Ni(H_2O)]^+/CH_4$.

Acknowledgements

This research was funded by Eusko Jaurlaritza (The Basque Government), and the Spanish Ministerio de Educación y Ciencia. O. L. would like to thank the Government of Navarre for a grant. The SGI/IZO-SGIker UPV/EHU (supported by Fondo Social Europeo and MCyT) is gratefully acknowledged for generous allocation of computational resources. Research in Berlin has been generously supported by the Fonds der Chemischen Industrie and the Deutsche Forschungsgemeinschaft: Cluster of Excellence "Unifying Concepts in Catalysis" coordinated by the Technische Universität Berlin.

References

1 For a recent, exhaustive review, see: H. Schwarz, *Angew. Chem., Int. Ed.*, 2011, **50**, 10096, and numerous references therein.
2 M. Schlangen, D. Schröder and H. Schwarz, *Angew. Chem., Int. Ed.*, 2007, **46**, 1641.
3 (*a*) A. Irigoras, O. Elizalde, I. Silanes, J. E. Fowler and J. M. Ugalde, *J. Am. Chem. Soc.*, 2000, **122**, 114; (*b*) Y. Dede, X. Zhang, M. Schlangen, H. Schwarz and M.-H. Baik, *J. Am. Chem. Soc.*, 2009, **131**, 12634.
4 For a recent review on remarkable nickel-mediated gas-phase reactions, see: M. Schlangen and H. Schwarz, *J. Catal.*, 2011, **284**, 126.
5 (*a*) A. D. Becke, *Phys. Rev. A: At., Mol., Opt. Phys.*, 1988, **38**, 3098; (*b*) A. D. Becke, *J. Chem. Phys.*, 1993, **98**, 5648; (*c*) C. Lee, W. Yang and R. G. Parr, *Phys. Rev. B: Condens. Matter*, 1988, **37**, 785.
6 Y. Zhao and D. G. Truhlar, *Theor. Chem. Acc.*, 2008, **120**, 215.
7 A. Schäfer, C. Huber and R. Ahlrichs, *J. Chem. Phys.*, 1994, **100**, 5829.
8 A. J. Wachters, *J. Chem. Phys.*, 1970, **52**, 1033.
9 P. J. Hay, *J. Chem. Phys.*, 1971, **66**, 4377.
10 K. Raghavachari and G. W. Trucks, *J. Chem. Phys.*, 1989, **91**, 1062.
11 J. S. Krishnan, J. S. Binkley, D. Seeger and J. A. Pople, *J. Chem. Phys.*, 1980, **72**, 650.
12 (*a*) J. A. Pople, R. Krishnan, H. B. Schlegel and J. S. Binkley, *Int. J. Quantum Chem.*, 1978, **14**, 545; (*b*) R. J. Bartlett and G. D. Purvis, *Int. J. Quantum Chem.*, 1978, **14**, 561; (*c*) K. Raghavachari, G. W. Trucks, J. A. Pople and M. Head-Gordon, *Chem. Phys. Lett.*, 1989, **157**, 479; (*d*) J. D. Watts, J. Gauss and R. J. Bartlett, *J. Chem. Phys.*, 1993, **98**, 8718.
13 M. J. Frisch, G. W. Trucks, H. B. Schlegel, G. E. Scuseria, M. A. Robb, J. R. Cheeseman, J. A. Montgomery Jr, T. Vreven, K. N. Kudin, J. C. Burant, J. M. Millam, S. S. Iyengar, J. Tomasi, V. Barone, B. Mennucci, M. Cossi, G. Scalmani, N. Rega, G. A. Petersson, H. Nakatsuji, M. Hada, M. Ehara, K. Toyota, R. Fukuda, J. Hasegawa, M. Ishida, T. Nakajima, Y. Honda, O. Kitao, H. Nakai, M. Klene, X. Li, J. E. Knox, H. P. Hratchian, J. B. Cross, V. Bakken, C. Adamo, J. Jaramillo, R. Gomperts, R. E. Stratmann, O. Yazyvev, A. J. Austin, R. Cammi, C. Pomelli, J. W. Ochterski, P. Y. Ayala, K. Morokuma, G. A: Voth, P. Salvador, J. J. Dannenberg, V. G. Zakrzewski, S. Dapprich, A. D. Daniels, M. C. Strain, O. Farkas, D. K. Malick, A. D. Rabuck, K. Raghavachari, J. B. Foresman, J. V. Ortiz, Q. Cui, A. G. Baboul, S. Clifford, J. Cioslowski, B. B. Stefanov, G. Liu, A. LIashenko, P. Piskorz, I. Komaromi, R. L. Martin, D. J. Fox, T. Ketih, M. A. Al-Laham, C. Y. Peng, A. Nanayakkara, M. Challacombe, P. M. W. Gill, B. Johnson, W. Chen, M. W. Wong, C. Gonzalez and J. A. Pople, *Gaussian 03, Revision C.02*, Gaussian, Inc. Wallingford, CT, 2004.
14 M. Valiev, E. J. Byalska, N. Govind, K. Kowalski, T. P. Straatsma, H. J. J. van Dam, D. Wang, J. Nieplocha, E. Apra, T. L. Windus and W. A. de Jong, *Comput. Phys. Commun.*, 2010, **181**, 1477.

15 (*a*) J. M. Mercero, J. M. Matxain, X. Lopez, D. M. York, A. Largo, L. A. Eriksson and J. M. Ugalde, *Int. J. Mass Spectrom.*, 2005, **240**, 37; (*b*) A. Irigoras, J. E. Fowlder and J. M. Ugalde, *J. Am. Chem. Soc.*, 1999, **121**, 8549.
16 (*a*) P. B. Armentrout, *Annu. Rev. Phys. Chem.*, 1990, **41**, 313; (*b*) P. B. Armentrout, *Science*, 1991, **251**, 175; (*c*) D. Schröder, S. Shaik and H. Schwarz, *Acc. Chem. Res.*, 2000, **33**, 139; (*d*) H. Schwarz, *Int. J. Mass Spectrom.*, 2004, **237**, 75.
17 (*a*) N. Koga and K. Morokuma, *Chem. Phys. Lett.*, 1985, **119**, 371; (*b*) N. A. Farazdel and M. Dupuis, *J. Comput. Chem.*, 1991, **12**, 276; (*c*) F. Jensen, *J. Am. Chem. Soc.*, 1992, **114**, 1596; (*d*) D. R. Yarkony, *J. Phys. Chem.*, 1993, **97**, 4407; (*e*) M. J. Bearpark, M. A. Robb and H. B. Schlegel, *Chem. Phys. Lett.*, 1994, **223**, 269; (*f*) K. M. Dunn and K. Morokuma, *J. Phys. Chem.*, 1996, **100**, 123; (*g*) J. M. Anglada and J. M. Bofill, *J. Comput. Chem.*, 1997, **18**, 992; (*h*) H. Schwarz, J. N. Harvey, M. Aschi and W. Koch, *Theor. Chem. Acc.*, 1998, **99**, 95.
18 M. Armélin, M. Schlangen and H. Schwarz, *Chem.–Eur. J.*, 2007, **14**, 5229.

